Tellus (2002), 54B, 735–748
Printed in UK. All rights reserved

TELLUS
ISSN 0280–6509

Seasonal variability of greenhouse gases in the lower troposphere above the eastern European taiga (Syktyvkar, Russia)

By K. SIDOROV[1]*, A. SOGACHEV[1], U. LANGENDÖRFER[2], J. LLOYD[3], I. L. NEPOMNIACHII[1], N. N. VYGODSKAYA[1], M. SCHMIDT[2] and I. LEVIN[2], [1]*Svertsov Institute for Evolutionary and Ecological Problems (IPEE), Leninskii pr. 33, 117071 Moscow, Russia;* [2]*Institut für Umweltphysik, University of Heidelberg (UHEI-IUP), Im Neuenheimer Feld 229, 69120 Heidelberg, Germany;* [3]*Max-Planck-Institut für Biogeochemie (MPI-BGC), Postfach 100164, 20146 Hamburg, Germany*

(Manuscript received 10 October 2001; in final form 17 June 2002)

ABSTRACT

A three year long record of regular vertical aircraft profiling for continuous atmospheric CO_2 mixing ratio measurements as well as for flask sampling to derive the climatology of other greenhouse gases (CH_4, SF_6 and N_2O), is presented. Measurements were undertaken in the lower troposphere between 100 and 3000 m over the eastern European taiga about 100 km south east of the city of Syktyvkar (61°24′N, 52°18′E). From the continuous profiles mean CO_2 mixing ratios were calculated for the atmospheric boundary layer (ABL) and for the "free troposphere" up to 3000 m. The amplitudes of the respective seasonal cycles are 22.1 ± 3.5 and 14.0 ± 2.1 ppm. ABL mixing ratios are generally larger than free tropospheric values during the winter period, and smaller during the summer due to the change of the continental biosphere from a source to a sink. The phasing of the seasonal cycles is slightly different between the two height intervals (by about 30 days), with the ABL extremes occurring earlier. Very abrupt concentration changes up to 8 ppm are observed in the free troposphere associated with changes in air mass origin. Mean CO_2 mixing ratios derived from flask samples at 3000 m compare well with the respective integrated values measured in the continuous profiles above the ABL ($\Delta CO_2 = 0.3 \pm 1.6$ ppm). CH_4 mixing ratios also show a pronounced seasonality, and winter time vertical gradients correlate well with those of CO_2. Similarly, SF_6 vertical gradients are correlated with CO_2 gradients possibly pointing to some anthropogenic origin of the boundary layer CO_2 signal during winter. N_2O and SF_6 also show a slight seasonality with almost the same phasing. The main reasons for the seasonality of both gases are probably transport processes with a possible contribution from stratosphere/troposphere exchange.

1. Introduction

The global atmospheric CO_2 observational network is largely biased towards maritime sites, and observations over the continents, in particular over the extended land masses of Eurasia, are very sparse. However, the question of partitioning the northern hemispheric CO_2 sink (Keeling et al., 1989; Tans et al., 1990) between continents and ocean can only be better assessed with a denser observational network, including more continental sites (Tans et al., 1996), and additional measurement of tracers for source apportionment, regular aircraft profiling (i.e. Nakazawa et al., 1997a), measurements of total column burdens and, in the near future, vertical profiles derived from satellite observations. The CO_2 mixing ratio in the lower troposphere over continental areas in mid-latitudes of the northern hemisphere should be directly influenced by

*Corresponding author.
e-mail: ks@lantech.ru

gas exchange with the vegetative surface below, but also by ground level anthropogenic emissions. Consequently, the CO_2 mixing ratio shows strong seasonal and also short-term variability, but the quantitative understanding of the processes involved, and their description by appropriate modeling (Chevillard et al., 2002a,b), is still at a preliminary stage. At least three processes are active over continental areas at the same time: (1) the intensive and diurnally varying CO_2 exchange with the biosphere at the ecosystem level, which also varies on small spatial scales in different landscapes, (2) atmospheric mixing processes which are driven by the boundary layer dynamics as well as by meso-scale circulation, large-scale advective transport and convective and turbulent processes, and (3) emissions from anthropogenic sources. The problem consists of a disentanglement of these components to finally derive (net) biological surface carbon fluxes from atmospheric CO_2 observations.

In this work we provide some examples of the interrelation between the variability of CO_2 mixing ratio with macro-synoptic conditions on the basis of regular vertical aircraft measurements in the lower troposphere up to 3000 m a.s.l. above the eastern European taiga. For the interpretation of the measurements, data were therefore classified in terms of the prevailing synoptic situation and origin of air mass. This is considered to provide a good indication of the origin and degree of transformation of the trace gas composition of the air mass, as strong surface interactions are expected here as a consequence of the extended land masses around the study area. The seasonal climatology of CO_2 within and above the ABL (further on referred to as "background") have been determined and are compared to other greenhouse gases such as CH_4 and SF_6.

2. Site description and techniques

2.1. Site description

Location. Regular flights were carried out about 100 km south east of the city of Syktyvkar, located in the Republic of Komi, Russia. The location over which all flights were undertaken (61°23′ 50″ N, 52°17′ 30″ E) was above the Vychegodsko-Mezenskoj Plain, about 200 km west of the base of the Ural Mountains (geographically speaking, the easternmost extent of Europe). Prevailing ground level heights in this region are 150–200 m above sea level (a.s.l). The highest elevations in the region are formed by a watershed plateau with a maximum height of 265 m a.s.l.

Climate. The climate is moderately continental with prevailing cyclone conditions and cloudy and rainy weather, long winters and short summer periods. A prominent feature of the climate are frequent intrusions of Arctic air masses from the Kara sea which are accompanied by cold north-easterly winds (Michkova, 1983). From long-term weather data available for Syktyvkar (1891–2001) minimum temperatures can even fall below 0 °C in July. This in turn can cause sharp decreases or even suspension of photosynthetic activity of the vegetation. During winter, these cold fronts can result in minimum temperatures as low as −49 to −55 °C. Cyclonic activity is especially strong during autumn and winter but weakens during spring and summer.

Soils and vegetation. For an area of ca. 100 km radius around the flight measurement location (in the following referred to as "immediate footprint"), podsolic soils dominate. These soils were formed over quaternary sediments of glacial and limno-glacial origin. Soils are seasonally frozen and temperate to cold. Natural fertility is low, with humus contents typically in the order of only 1.5%. Besides podsolic soils, swampy–podsolic soils are also typical for the area. Peat bogs are formed in wet and poorly drained regions (Kogubov and Toskaev, 1999). The vegetation cover is dominated by medium size young pine forest (*Pinus sylvestris* L.) with intermediate small cuttings. Also, it is important to note that, for the immediate footprint as well as for the whole Republic of Komi, wetlands occupy a significant proportion of the land cover (Kogubov and Toskaev, 1999). These are especially prevalent in the region north of the study site.

Ecological situation. The average population density of the Republic of Komi is two persons per km^2 with a total population in the capital Syktyvkar of 160 000. The city is a mostly administrative centre with CO_2 emissions from burning of fossil fuels largely from transportation as well as from domestic heating (hard coal) during the winter period. These are probably the most significant anthropogenic contamination factors in the study area. The only large industrial enterprise is a cellulose-paper factory, the largest in Europe, 18 km north east of the city. Emissions from this anthropogenic point source can potentially influence trace gas measurements during aircraft flights,

located at a distance of about 120 km to the south east.

2.2. Sampling techniques

Sampling. Regular aircraft flights were performed every 2–4 weeks with local Antonov-AN2 bi-plane aircraft from 100 to 3000 m above ground elevation. Flights commenced in May 1998 and at the time of writing are ongoing. Data presented here cover the period May 1998 to May 2001. Flights were generally performed between 0700 and 1200 h local time. Separate air intake lines (6 mm dekabon tubing, ca. 10 m long) for continuous CO_2 measurements and for flask sampling systems were installed in the wings of the aircraft as far away as possible from engine exhaust. Vertical profiles of continuous CO_2 soundings as well as temperature and relative humidity were measured. The NDIR (non-dispersive infrared) system for continuous CO_2 measurement was designed by the Max Planck Institute for Biogeochemistry, Jena (Lloyd et al., 2002). We used a special "low-noise" flow- and temperature-controlled LiCor-6152 infrared gas analyser provided by the manufacturer, for which the precision of measurements was estimated to better than 0.1 ppm. With the regular in-flight calibrations we estimate an overall accuracy of better than 0.5 ppm (see also flask/NDIR comparison in Fig. 2). Two standard gases were regularly used during the flight for re-calibration of the instrument. Carbon dioxide mixing ratios in these standard gases were calibrated at the Institut für Umweltphysik, University of Heidelberg (UHEI-IUP); they are related to the primary WMO CO_2 mole fraction scale maintained at NOAA/CCGG, Boulder, CO. Calculation of CO_2 mixing ratios is described by Lloyd et al. (2002). In addition to the continuous CO_2 measurements, duplicate whole-air flask samples were collected at 2000, 2500 and 3000 m a.s.l. and analysed at UHEI-IUP for CO_2 mixing ratio and stable isotope ratios in CO_2, as well as for CH_4, N_2O and SF_6 mixing ratios (Levin et al., 2002). Samples were collected into 1 L cylindrical flasks made of Pyrex glass with PFA O-ring valves (Glass Expansion, Australia) at both ends. Before shipment to the sampling site, for "conditionning" flasks were flushed with dry air and pressurised to 0.8 atm above ambient pressure. In the aircraft for sampling, flasks were flushed for more than 5 min at a flow rate of ca. 4 L min^{-1}, and pressurised to 1 atm above ambient pressure at final filling (pump: KNF-Neuberger, Germany, N86KNDC with EPDM membrane). Drying of the air was performed via magnesium perchlorate [for tests of the drying system, see Levin et al. (2002)]. For the set up of the flask sampling system see Ramonet et al. (2002).

Flask analysis and calibration. Flask analysis for CO_2 was performed by gas chromatography (GC) with a nickel catalyst for conversion of CO_2 to CH_4, and a flame ionization detector (FID). Methane was analysed directly by GC-FID (Levin et al., 1999), while N_2O and SF_6 mixing ratios were measured by the GC electron capture detector technique (ECD) (Maiss et al., 1994; Schmidt et al., 2001). CO_2 mixing ratios are reported in the WMO CO_2 mole fraction scale maintained at NOAA/CCGG, Boulder, CO, USA. Laboratory primary standards (CO_2 in natural air) were obtained from NOAA/CCGG, and are periodically re-calibrated (last re-calibration in 1998). Methane mixing ratios are related to the NOAA/CCGG scale. For N_2O, no internationally agreed calibration scale is available. Flask data are, therefore, preliminarily linked to the SIO93 scale maintained at the Scripps Institution of Oceanography for the ALE/GAGE and AGAGE programs (Weiss et al., 1981; Prinn et al., 2000; Schmidt et al., 2001) with an accuracy of better than ± 1 ppb. Data for SF_6 are reported relative to a diluted gravimetric standard gas provided by Messer Griesheim, Mannheim, Germany. The dilution procedure is described by Maiss et al. (1996). Its absolute accuracy is better than 1%. As described by Levin et al. (2002), all CO_2 and N_2O mixing ratios from flask samples have been corrected for drift during storage. For CO_2, an initial offset of -0.06 ppm, and a subsequent drift of -0.0012 ppm per day of storage was corrected for; for N_2O, the drift correction was 0.0035 ppb per day of storage. Flasks from two flights (4 and 22 October 1999) which were identified as contaminated during sampling through highly elevated CO_2 and CH_4 mixing ratios have been rejected from the data set; all other flask measurements were retained. Flask pairs were analysed in the laboratory on different days to minimize possible systematic biases. The mean standard deviation and its variability of measurements on the duplicate flasks was 0.085 ± 0.083 ppm for CO_2, 1.6 ± 1.4 ppb for CH_4, 0.21 ± 0.16 ppb for N_2O and 0.009 ± 0.008 ppt for SF_6. These pair reproducibilities are compatible with the precision of individual measurements determined through duplicate analyses of samples such as test flasks filled with air of known mixing ratios and high-pressure tanks. The absolute accuracy of the CO_2 measurements in terms of comparability to other measurements in the

GAW/WMO network is better than 0.3 ppm in the case of the flask data and better than 0.5 ppm in the case of the continuous NDIR data.

3. Results and discussion

For the analysis of the temporal variability of atmospheric CO_2 over the northern European taiga the data from 43 aircraft flights were used. Note that from June 1998 until March 1999, only flask data and meteorological parameters but no continuous NDIR CO_2 measurements are available.

3.1. Seasonal variability of atmospheric CO_2

As an integrated parameter to derive the CO_2 content in the lower troposphere, the average CO_2 mixing ratios inside and above the boundary layer up to the highest flight level at 3000 m above ground were calculated from the continuous NDIR profiles (Figs. 1 and 2). The boundary layer height (HBL) was also determined. Because of the absence of data on vertical distribution of a wind, HBL was defined as the height of a change in the gradient of potential temperature. The lowest height at which the occurrence of a positive gradient of the air temperature (inversion) was always the boundary layer height (Byzova and Ivanov, 1989).

Harmonic fit curves were calculated through the three different data sets (with measurements available at the same flight dates) using the procedure described by Nakazawa et al. (1997b). Regular seasonal changes of the CO_2 mixing ratio were observed, associated with net photosynthetic activity during the vegetative period and net soil and plant respiration fluxes to the atmosphere during autumn and winter. Above the ABL up to 3000 m the lowest mixing ratio of 356 ppm was observed during summer 1999, and maximum values as high as 377 ppm were seen in winter. As derived from the harmonic fit curves, the shape of the seasonal cycle within the atmospheric boundary layer is similar to that of the free troposphere. The mean amplitude is, however, larger by about 50% (the mean amplitude from the harmonic fit curve is 22.1 ± 3.5 ppm compared to 14.0 ± 2.1 ppm above the boundary layer). The phasing of the seasonal cycle is also slightly different, with the ABL maximum (Julian day 32) preceding that of the "free troposphere" (Julian day 72) by 40 days and the ABL minimum (Julian day 216) preceding that of the "free troposphere" (Julian day 231) by 15 days. For the three years of observations the phasing of the seasonal cycles varies by up to 30 days. This is caused by both the low frequency of flights and the considerable variability of air mass history (see Section 3.2).

The lower mean CO_2 mixing ratio inside the boundary layer compared to the free troposphere during daylight hours in summer reflects the strong photosynthetic activity of plants during this time of the year. In autumn and early winter, the higher CO_2 mixing ratio

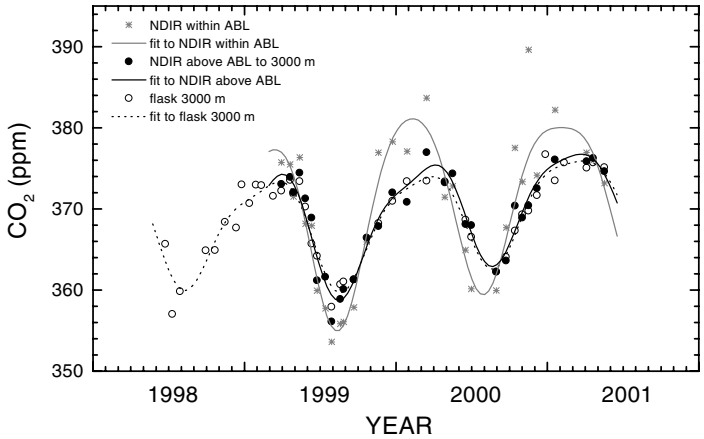

Fig. 1. Temporal evolution of atmospheric CO_2 calculated from the continuous NDIR profiles from data measured within the ABL and above the ABL up to 3000 m. Also included are the results from flask samples collected during the same flights at the 3000 m level. The continuous lines are harmonic fit curves calculated through the respective data records according to Nakazawa et al. (1997b).

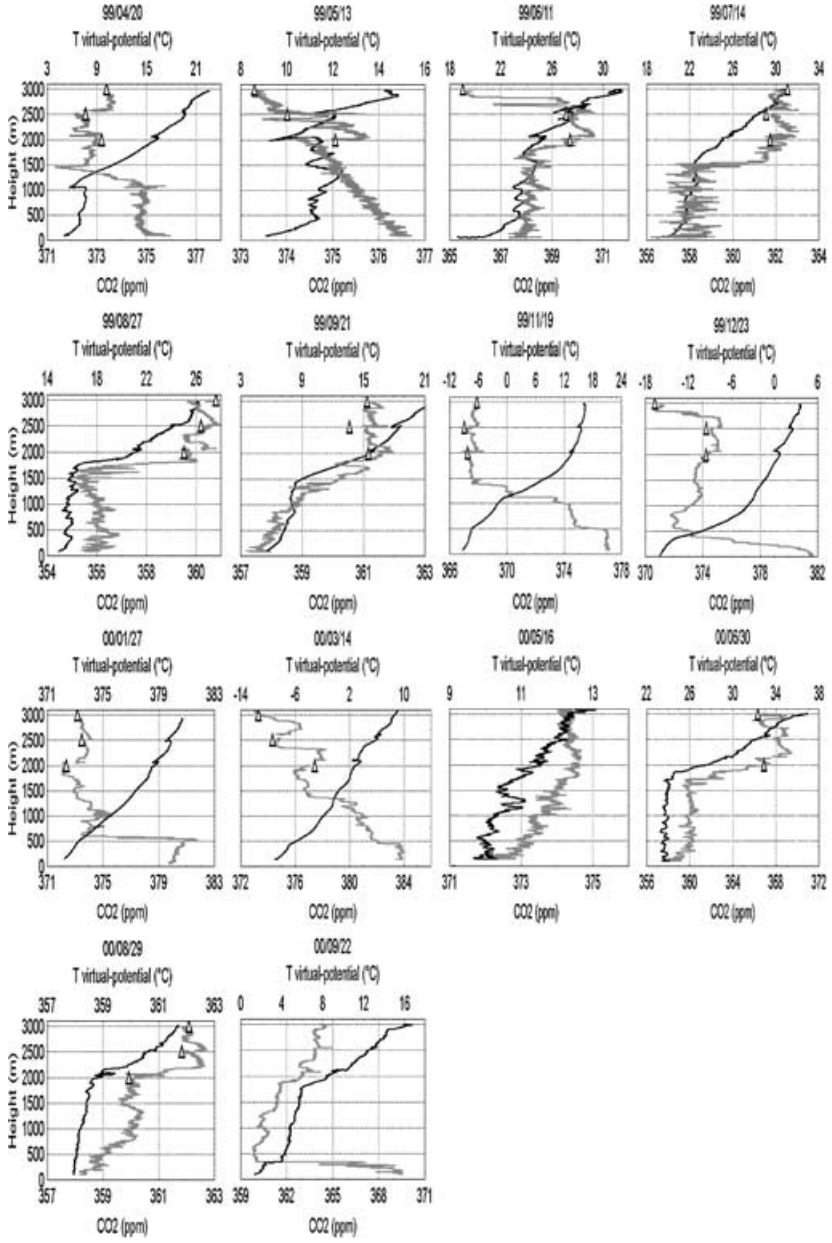

Fig. 2. Selected vertical profiles of CO_2 mixing ratio (grey line), virtual-potential temperature (black line), and CO_2 derived from flask samples (triangle). The seasonal cycle of the height of the atmosphere boundary level (HBL) is also shown (dotted line).

in the boundary layer is mainly due to net ecosystem respiration of plants and soils. The reason for a persistent CO_2 concentration gradient during the winter with higher levels in the boundary layer under conditions of permanent snow cover and air temperatures as low as -50 °C is not yet fully understood. However, even under these conditions, soil respiration through snow cover may be significant if soil temperatures are

around 0 °C, due to the insulation effects of the snow cover (Zimov et al., 1993; Shibistova et al., 2002). The strong correlation between CO_2 and CH_4 gradients (and also between CO_2 and SF_6 gradients) during winter does, however, also point towards anthropogenic sources for these three trace gases (see Section 3.3).

Also plotted in Fig. 1 are the CO_2 mixing ratios derived from flask samples at the 3000 m level, which for all flights were collected above the atmospheric boundary layer, i.e. in the free troposphere. The harmonic fit curve through these flask data (seasonal amplitude of 12.4 ± 2.0 ppm, Julian day of maximum 68, Julian day of minimum 232), within the uncertainty due to the synoptic variability (see Section 3.2) and the sparseness of data, is indistinguishable from the curve fitted through the integrated NDIR data for the free troposphere, this being the mean mixing ratio between the top of the boundary layer and 3000 m. For individual flights the mean difference between the NDIR free troposphere integrated value and the flask data at 3000 m is 0.3 ± 1.6 ppm, with maximum deviations not exceeding ± 3.5 ppm. This agreement is promising, as it suggests that flask sampling alone, at least concerning the seasonal CO_2 cycle at the 3000 m height level, may provide a rather representative climatology in the absence of continuous data. Note, however, that the CO_2 variability around the mean seasonal cycle can be large due to different origin of air masses sampled during different flights (Section 3.2).

Figure 2 shows the vertical distribution of CO_2 mixing ratios measured with the NDIR system as well as the virtual potential temperature in high vertical resolution during selected flights. Also shown are the results from flask samples at 2000, 2500 and 3000 m. Again the very good agreement of CO_2 mixing ratios between data derived from continuous NDIR profiles and analyses on flask samples is illustrated. Except for one case which was rejected from this analysis, differences between the two measurements did not exceed ± 1 ppm. The mean difference between the continuous in-site CO_2 measurement at the respective height and during the last minute of flask flushing and pressurizing and the flask measurement is 0.42 ± 0.33 ppm for 2000 m, 0.53 ± 0.36 ppm for 2500 m and 0.14 ± 0.68 ppm for 3000 m. These differences are within the estimated uncertainty of the NDIR measurement.

In Fig. 2 the seasonal dynamics of the height of the boundary layer is also marked. This is further shown in Fig. 3, where the mean seasonal cycle of the boundary layer height above ground, derived from the data of all flights of the three year long period from 20 May 1998 to 17 May 2001 is presented. As mentioned above, the convective boundary layer height depends on many factors, and therefore there is no smooth seasonal course of the ABL. Generally the heights are in the order of only a few hundred metres in autumn and winter and of about 1000–1500 m during spring and summer. However, low heights, comparable to those observed in winter, are also sometimes found during the summer season. These situations are generally related to cyclonic weather conditions when continuous cloud cover suppresses radiative heating with associated suppressed vertical turbulence. As a rule, in such cases the ABL height is at the base of the lowest cloud layer. Note, however, that the ABL height also changes during the course of the day, particularly in summer, and flights were performed between 7 and 15 pm.

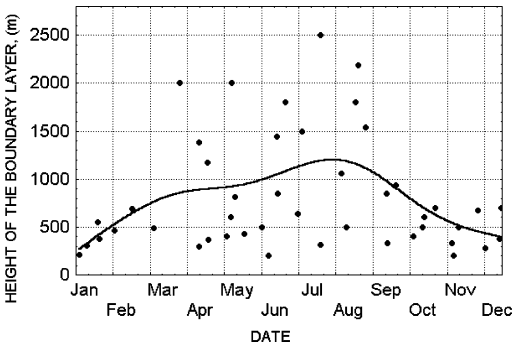

Fig. 3. Mean seasonal cycle of the height of the boundary layer derived from all aircraft flights between 20 May 1998 and 17 May 2001 at Syktyvkar. The solid line is a sixth-order polynomial fit through the data.

3.2. Synoptic conditions

For an estimation of influence of synoptic conditions on distribution CO_2 in the lower troposphere we used three parameters: (1) type of weather conditions; (2) thermal stratification of an atmosphere; and (3) direction of motion of air mass.

In total, about 60% of the flights were carried out at anticyclone weather situations, while about 40% were during cyclone situations. About 45% of the cases experienced westerly and north-westerly air masses, while during about 55% of the flights air came from other directions. During measurements we observed about 30 various types of weather. However, in this work we have divided all types of weather into two classes: anticyclone (Az) and cyclone (Zn) as direction of vertical streams (Table 1).

Table 1. *The mean CO_2 mixing ratios, as calculated from the NDIR profiles, within classification of the individual flights in terms of meteorological situation together with the boundary layer heights derived from the vertical profile of the virtual potential temperature. The mean CO_2 mixing ratios within the ABL as well a in the "free troposphere" (i.e. above the ABL up to 3000 m) are also given*

Date and local time of Flight	Wind direction in free troposphere	Height of boundary layer (m) above ground	CO_2 ABL (ppm)	Stdd. Dev. (ppm)	CO_2 free troposphere (ppm)	Stdd. Dev. (ppm)
Anticyclone, stable stratification						
990729 13-28	W	314	353.60	0.36	356.13	1.67
991119 13-23	NE	500	376.94	0.16	367.86	0.82
991223 11-06	N	380	378.28	2.65	372.02	1.16
000922 08-30	N	330	367.69	1.76	363.61	0.66
001205 14-00	N	670	374.13	1.53	372.56	1.78
Anticyclone, unstable stratification						
990611 12-23	N	500	367.93	0.26	368.93	1.43
990624 15-34	S	850	359.93	0.29	361.20	1.28
990827 13-38	NW	1800	356.07	0.54	360.10	0.39
990921 12-52	NE	845	357.87	0.28	361.30	0.40
000516 13-36	SW	600	372.82	0.36	374.37	0.16
000630 09-32	E	1800	360.14	0.83	368.00	1.08
000829 12-55	NW	2190	359.94	0.77	362.28	0.24
001013 17-22	NE	400	377.52	0.24	370.39	3.25
001115 11-40	NW	200	389.62	2.18	370.43	0.51
Cyclone, stable stratification						
990420 12-52	N	300	375.49	0.34	373.92	0.88
990513 14-37	SW	400	376.33	0.14	374.45	0.92
990527 12-12	W	430	368.17	0.38	371.28	0.76
991022 12-30	N	600	365.93	0.25	366.46	0.79
000127 10-11	S	550	377.09	0.28	370.85	1.27
000314 11-28	S	490	383.66	0.33	376.98	2.47
010118 10-10	N	310	382.18	0.25	376.09	2.20
010404 14-43	NW	2000	376.94	0.37	375.86	0.60
Cyclone, unstable stratification						
990428 12-16	N	370	371.53	0.21	372.04	0.80
990714 10-26	NW	1500	357.74	0.61	361.61	0.76
990819 11-33	SW	500	355.83	0.44	358.88	1.97
000427 13-32	W	1175	371.45	0.38	373.26	0.57
000616 13-24	SW	200	364.92	0.87	368.10	0.65
001031 13-30	NE	700	373.34	0.59	368.90	0.34
010420 12-13	W	1382	375.98	0.25	376.27	0.41
010517 13-38	W	2000	373.19	0.28	374.63	0.49

Inside a boundary layer some sublayers may to be placed; therefore we have calculated an average temperature gradient in the boundary layer: if it is more than 0.98 °C per 100 m there is unstable stratification; if less, stable; if equal, neutral stratification (Brutsaert, 1985).

For classification of the flights into the different synoptic situations and to determine the mean wind direction of the air masses, the pressure fields at the surface and at the 500 mbar level were used. The results are summarised in Table 1.

We have shown vivid examples of the influence of the chosen parameters on CO_2 distribution in Fig. 4.

Significant differences in absolute CO_2 mixing ratios are observed in the vertical profiles in air masses of different origin even sampled less than two weeks apart (Table 1). Mean CO_2 differences over the entire profile were observed to be as large as 8 ppm, as shown in the examples of 11 June and 24 June 1999 (Figs. 4a–c). As is illustrated in Figs. 4d–f, and observed on a number of other occasions, in cyclonic situations (16 June 2000) the height of the boundary

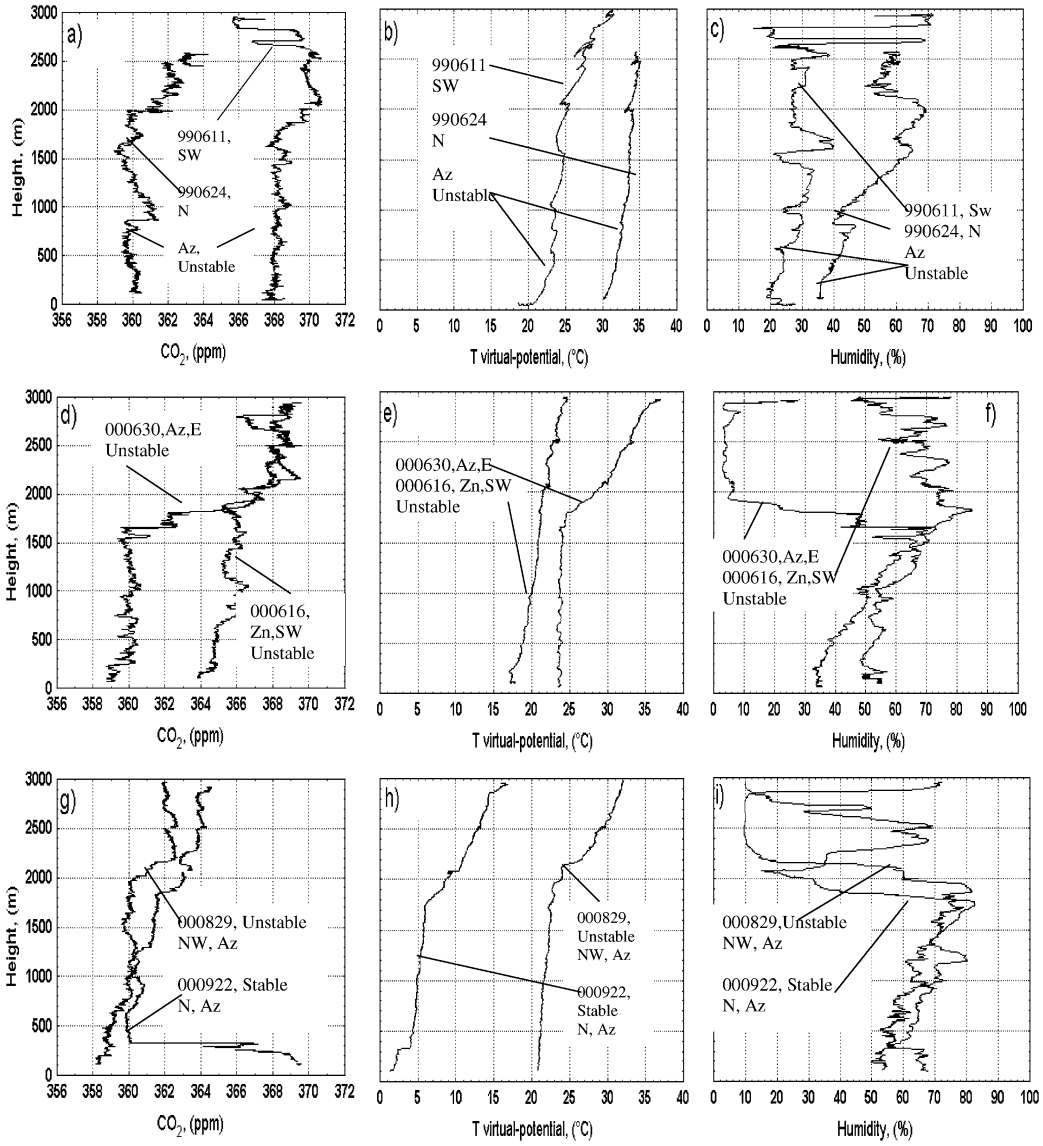

Fig. 4. Vertical profile of the CO_2 mixing ratio (a, d, g), virtual-potential temperature (b, e, h) and humidity (c, f, i) for various air mass origins and meteorological situations. Upper panel: a, b and c compare the situations of 11 and 24 June 1999, two anticyclone (Az) situations with unstable stratification but different wind directions. The mean CO_2 mixing ratios differ by 8 ppm between the two profiles. Middle panel: d, e and f cyclone (Zn) and anticyclone (Az) conditions of 16 and 30 June 2000 also during unstable stratification. The boundary layer height on 16 June was 200 m, while it was at 1800 m on 30 June. Lower panel: g, h, and i unstable and stable temperature stratifications of 8 August and 9 September 2000. Height of boundary layer 2190 of 8 August 2000 and 330 m of 9 September 2000.

layer tends to be lower (at about 200 m) than when an anticyclonic situation prevails (30 June 2000; ABL at 1800 m). This example confirms our knowledge about powerful rising streams in an anticyclone. In case of stable thermal stratification vertical mixing of air is complicated. Hence, the height of a boundary layer should be less than in the case of an unstable atmosphere (Figs. 4g–i).

It should also be remembered that one of the most important properties of the boundary layer is its role as a "buffer zone". By this we mean that heat, moisture but also pollution from surface emissions are usually initially captured within the ABL. Transport of these substances (in our case CO_2) to other layers within the lower troposphere is, however, frequently observed. One transport mechanism is the daily cycle of the vertical movement of the boundary layer height. In the afternoon with increasing convective mixing the contents of the boundary layer are pumped upwards to the free troposphere and remnants stay there during night, or are transported further up through slow synoptic ascending movements. Another mechanism of boundary layer ventilation is associated with a "break-up" of the boundary layer as a result of large-scale thermal instability associated with the occurrence of ascending processes penetrating into all layers of the troposphere. Therefore, a stepwise change of the vertical CO_2 concentration profile will not necessarily coincide with the height of the actual boundary layer (Matveev, 1984). This is visible in an example of winter–spring structures when the height of the boundary layer is estimated to 500 m, but with uniform CO_2 concentration to a level of more than 1000 m (c.f. Fig. 2, profile of 20 April 1999). Similarly, low heights of the boundary layer are frequently observed in the summer, with concurrent high CO_2 concentrations at heights between 1900 and 2800 m (Fig. 2, profile of 11 June 1999). Nevertheless, we can still conclude that the height of the boundary layer is generally higher in the summer than it is in the winter due to vertical mixing by convective turbulence (Fig. 3).

In the interpretation of seasonal and spatial changes of CO_2, horizontal advection also has to be taken into account. To explain the variability of CO_2 concentrations observed, we therefore used the data on wind direction to help classify the profiles (Table 1). In Fig. 4a–c the vertical profiles of CO_2, virtual potential temperature and humidity are shown for two anticyclone situations and unstable conditions in the middle of the vegetation period (June 1999). Inspecting back trajectories of the respective days in June 1999 [for a description of the calculation of back trajectories see Levin et al. (2002)] from this example it can be seen that in conditions of strong northerly flow (see trajectory of 11 June 1999 for 2500 m in Fig. 5a), CO_2 concentration is higher by about 8 ppm throughout the whole profile than during air mass flow from initially southern direction and a residence time of about 3 days over mid latitude land surface (see trajectory of 24 June 1999 in Fig. 5b). Such changes are almost in the same order as the amplitude of the seasonal cycle (i.e. in the boundary layer of 22.1 ± 3.5 ppm, and in the free troposphere of about 14.0 ± 2.1 ppm). Likely, the large difference of concentrations between northerly and south-westerly air masses are the result of strong uptake of CO_2 by the continental biosphere in early summer. During early June, CO_2 mixing ratios in the Arctic are still almost at their spring maximum. Similar large variations from flight-to-flight in early summer were also observed above Zotino in central

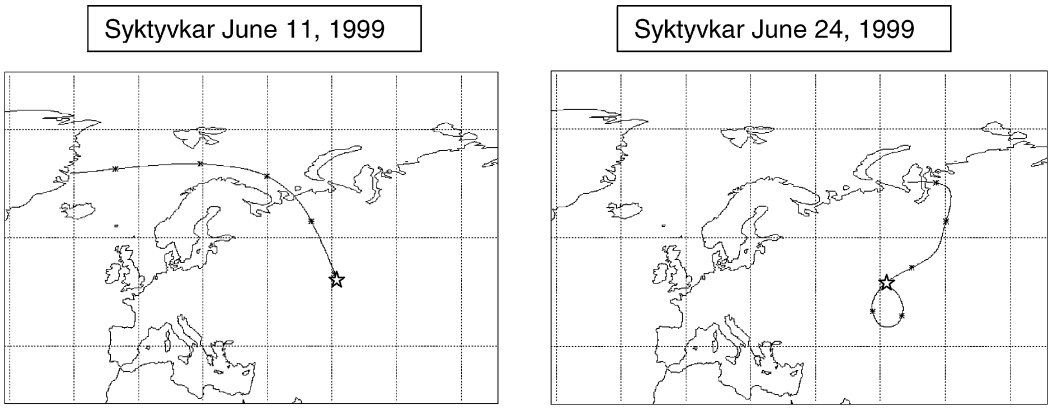

Fig. 5. Five day back trajectories calculated for the 2500 m levels for the flights of 11 and 24 June 1999. The large star is plotted at the sampling site, the small stars show the positions of the trajectories on respective days at midnight.

Siberia by Lloyd et al. (2002). As for the situation discussed here, in Zotino they were related to the rapid transition of the arctic vegetation to an actively photosynthesising state around this time of the year and to large differences in air mass origin.

3.3. Comparison of CO_2 with other greenhouse gases

Due to the more complex measurement techniques required, concentration analysis of other greenhouse gases, CH_4, N_2O and SF_6, were made only on flask samples, and Fig. 6 shows the concentration measurements of CO_2, CH_4, SF_6 and N_2O derived from the flask samples collected at 2000, 2500 and 3000 m. To assist in interpretation of the data, harmonic fit curves calculated through the 3000 m data according to Nakazawa et al. (1997b) are also shown. All four components show distinct seasonal cycles, most regular at 3000 m height. It is also clear that the lower level concentrations show much more variability. In the case of CO_2, this variability has already been attributed to

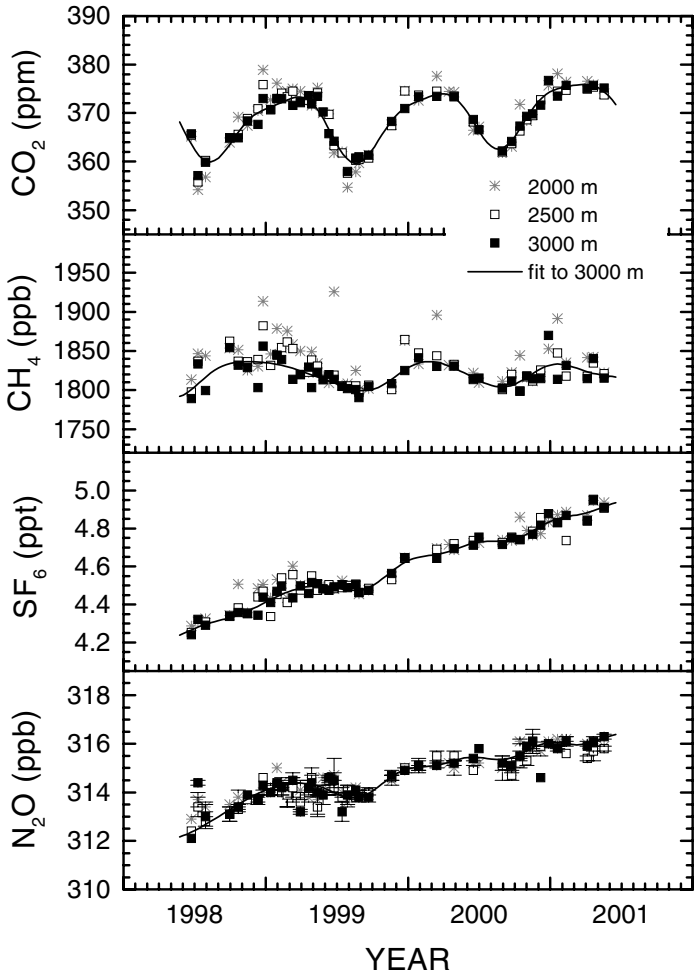

Fig. 6. Temporal evolution of greenhouse gases mixing ratios derived from flask samples collected at 2000, 2500 and 3000 m. The solid lines through the data are harmonic fit curves calculated through the 3000 m data which for all flights represent measurements above the actual boundary layer in the "free troposphere". In most cases (except for N_2O) the error bars (pair reproducibility) are smaller than the symbols and not shown here.

the seasonal biogenic CO_2 exchange and possible influence from anthropogenic emissions. In the case of CH_4, a particularly larger scatter of the lower level flask data is observed, especially during winter. In the study area, CH_4 has strong natural sources from wetland emissions, but these might be expected to be mainly restricted to the summer and autumn periods (Panikov and Dedysh, 2000). Besides these natural emissions, anthropogenic sources from natural gas production and distribution but also from agriculture and domestic wastes deposits may play a role all year round. Inspection of the respective vertical differences between 2000, 2500 and 3000 m for both gases, CO_2 and CH_4 yields a very good correlation for the winter profiles (Fig. 7a). As expected, during the summer, when local methane emissions are strong but CO_2 has a net sink at ground level, the correlation between the CO_2 and CH_4 gradients disappears. The slopes of the regression lines of about 11 ppb CH_4 per ppm CO_2 during winter derived here from vertical trace gas gradients are very similar to those which can be inferred from the CO versus CO_2 and CO versus CH_4 relationships presented by Lloyd et al. (2002) for winter flights in central Siberia (Zotino). This slope also falls between the observations at Alert of 14 ppb CH_4 per ppm CO_2 (Worthy et al., 1994) and measurements in western Europe at the Schauinsland station, where a mean ratio of 7.8 ppb CH_4 per ppm CO_2 was found for the winter season (Schmidt et al., 1996). To some degree the difference between the ratios in the present studies and those of Worthy et al. (1994) and Schmidt et al. (1996) may be attributable to slightly different methodologies of calculation. Both the latter studies analysed their data in terms of temporal changes of absolute CO_2 and CH_4 values, whereas the current study and that of Lloyd et al. (2002) have examined the relationship in terms of within flight deviations from either the minimum observed values for each flight (Lloyd et al., 2002) or relative to the observed concentrations at 3000 m (Fig. 7). An alternative explanation for this difference between western Europe, northern taiga, and the Arctic may be a decreasing contribution of soil respiration and fossil fuel CO_2 to the CO_2 offset.

Besides CH_4 and CO_2, also the SF_6 mixing ratio at the 2000 and 2500 m levels shows considerable scatter during winter, this being most pronounced during 1999 (Fig. 6). SF_6 is a chemically very stable and purely anthropogenic greenhouse gas, with about 80% of the global SF_6 release presumably from leakage in

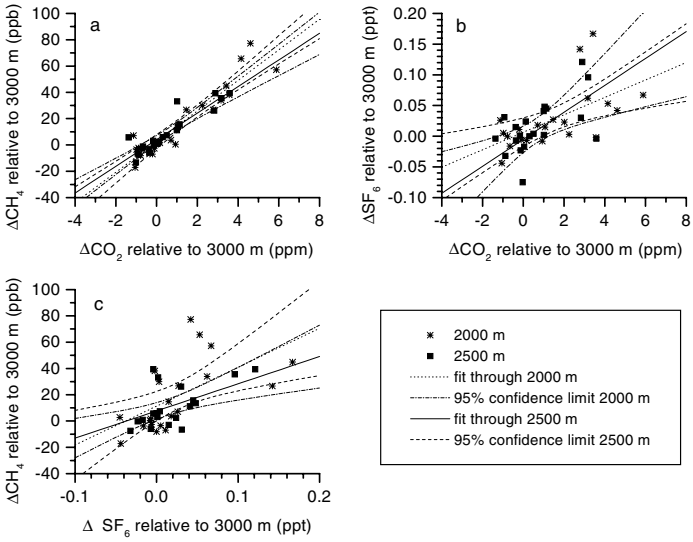

Fig. 7. Correlation between greenhouse gases mixing ratios derived from flask measurements for the winter half-year differences between 3000 m and 2000 and 2500 m for (a) CH_4 and CO_2 with slopes in ppb CH_4 per ppm CO_2 for: 2000 m, 11.6 ± 1.0, R^2–0.88; 2500 m, 10.1 ± 1.0, R^2–0.85; (b) SF_6 and CO_2 with slopes in ppt SF_6 per ppm CO_2 for: 2000 m, 0.014 ± 0.007, R^2–0.36; 2500 m, 0.022 ± 0.007; R^2–0.36; (c) CH_4 and SF_6 with slopes in ppb CH_4 per ppt SF_6 for: 2000 m, 296 ± 94, R^2–0.35; 2500 m, 207 ± 59, R^2–0.41. In all three cases the slopes for the 2000 and 2500 m samples are indistinguishable.

electrical insulation and switching, and about 20% from degassing and purifying of molten reactive metals (Maiss and Brenninkmeijer, 1998). Destruction of SF_6 occurs only in the high stratosphere and in the mesosphere. Since the 1970s, atmospheric SF_6 has been increasing globally at a rate of more than 6% per year (Maiss et al., 1996; Geller et al., 1997). Our measurements from the last three years (1998–2001) show a mean increase rate of 5% per year. Similar to CH_4 during winter, SF_6 differences between 2000, 2500 and 3000 m heights show a correlation ($R^2 = 0.36$) with the respective CO_2 differences. This result suggests that, as for SF_6, the positive CO_2 gradients in winter are, to a significant extent, due to different amounts of CO_2 from anthropogenic sources being present at the different heights. In concurrent studies by Lloyd et al. (2002) and Ramonet et al. (2002), the atmospheric CO mixing ratio has been used as a tracer for anthropogenic contamination of air samples. At the time of this study, unfortunately, CO measurements were not possible at UHEI-IUP. The results of Fig. 7b, however, indicate that SF_6 measurements may also be used as such an indicator for air masses of anthropogenic origin. One should, however, keep in mind that the source distribution of SF_6 and anthropogenic CO_2 may be different at least on the regional scale.

Figure 6 also shows the N_2O mixing ratios measured in the flask samples from Syktyvkar. We observe here a mean increase rate in the free troposphere (3000 m) of 1.2 ppb per year. The principal source of N_2O is considered to be tropical soils, but also natural soils in the temperate zone can be significant sources of N_2O to the atmosphere (Ehhalt et al., 2001). The largest anthropogenic emissions are associated with fertilised agricultural soils, but also industrial emissions, i.e. from fertiliser production, cannot be neglected. Similar to SF_6, N_2O has no sinks in the troposphere. N_2O is destroyed by photolysis at wavelengths between 180 and 230 nm in the stratosphere. Our data from vertical aircraft sampling show no vertical gradient in the troposphere between 2000 and 3000 m. Also the scatter of the data is similar at all three heights and mainly attributed to measurement uncertainty. Although future observations at lower elevations have to confirm this assumption, from the missing vertical gradient between 2000 m and 3000 m we conclude that in the immediate footprint (ca. 100 km around the sampling site) but probably also in the larger catchment area (ca. 500–1000 km distance) of the aircraft flights there are most probably only very minor N_2O sources not significantly affecting the aircraft measurements.

Our N_2O observations show a quite regular seasonal cycle with maximum concentrations during winter and spring and a minimum in autumn. The phasing of the seasonal cycle of N_2O is very similar to that of SF_6. The purely anthropogenic SF_6 sources are not known to vary with season. For N_2O, natural and anthropogenic emissions from soils are generally at a maximum during spring and summer (Flessa et al., 1995; Schmidt et al., 2001) which should give rise to maximum concentrations in the free troposphere in summer and autumn. By contrast, concentrations of both gases, N_2O and SF_6, tend to be more or less constant or even slightly decreasing during summer. Therefore, rather than being due to seasonally varying sources, the observed seasonality of both gases is more likely due to atmospheric mixing processes, with a possible contribution of seasonal stratosphere/troposphere exchange which peaks in spring and early summer (Appenzeller et al., 1996). Air intrusion from the stratosphere in spring might well induce a seasonality with the observed phasing, as the concentrations of both gases strongly decrease with height even in the lower stratosphere (Harnisch et al., 1998; Strunk et al., 2000).

4. Conclusions

The findings of our study clearly show that observed trace gas mixing ratios in the free troposphere over the continent, where large sources and sinks are active, exhibit a quite large variability. They have thus to be interpreted in the context of both atmospheric vertical mixing driven by the boundary layer dynamics and large and mesoscale circulation patterns. It could be shown that by means of vertical profiling of the virtual potential temperature, as well as by back trajectory analyses, these transport effects on the observed mixing ratios can effectively be separated. In the context of long-term monitoring to derive the trace gas climatology in the free troposphere, our comparison between the integrated high-resolution in-situ CO_2 mixing ratio above the ABL and spot flask sampling at selected height levels suggests that flask sampling well above the ABL yields reasonable values for the free troposphere. However, in order to derive a representative trace gas climatology, one has to keep in mind that the frequency of flights must be high enough to compensate for the large variability of concentration signals due to changes in air mass origin during individual flights. Moreover, for a reliable interpretation of CO_2 signals, besides meteorological information, a

multi-tracer approach as presented here by additional flask analysis of CH_4, SF_6 and N_2O provides valuable information concerning source apportionment. In particular, it could be shown that, at least when considering large spatial scales such as in this study of aircraft measurements, SF_6 may also serve as a tracer to identify anthropogenically influenced air masses, and therewith partly replace the classical trace gas CO where these data are missing.

5. Acknowledgements

Our thanks are expressed to all who helped in gathering the information, and with the preparation of the present work: the staff of the hydrometeorological centre of Russia of L.I. Il'kun, to the organisers of the flights in Syktyvkar, V.V. Vlasovu, N.M. Kopejkinu, V.A. Svjatovets, to the commander of the summer crew L.N. Myshkinu, to pilot L.V. Pishchal'nikovu, and also to the technicians V.S. Gabovu, V.A. Portnjaginu, V. V'juhinu. D. Zolotuhin, who have helped with the organisation and realisation of the flights. We also thank N. Smoljar and K. Thomas, who helped with Russian–English translations, and two anonymous reviewers for their helpful suggestions to improve the quality of this manuscript. This project has been partly funded by the European commission under ENV4-CT-97-0491 and by the Max-Planck-Gesellschaft, München, Germany. The most important thing now and in the future is that the number of safe starts is equal to the number of safe landings.

REFERENCES

Appenzeller, C., Holton, J. R. and Rosenlof, K. H. 1996. Seasonal variation of mass transport across the tropopause. *J. Geophys. Res.* **101**, D10, 15071–15078.

Brutsaert, W. 1985. *Evaporation into the atmosphere. Theory, history and applications*. Gidrometeoizdat, Leningrad, 351 pp.

Byzova, N. L. and Ivanov, V. N. 1989. Turbulence in boundary level. Gidrometeoizdat, Leningrad, 230 pp.

Chevillard, A., Ciais, P., Karstens, U., Heimann, M., Schmidt, M., Levin, I., Jacob, D. and Podzun, R. 2002a. Transport of ^{222}Rn using the regional scale model REMO: A detailed comparison with measurements over Europe. *Tellus* **54B**, this issue.

Chevillard, A., Karstens, U., Ciais, P., Lafont, S. and Heimann, M. 2002b. Simulation of atmospheric CO_2 over Europe and Western Siberia using the regional scale model REMO. *Tellus* **54B**, this issue.

Ehhalt, D., Prather, M., Dentener, F., Derwent, R., Dlugokencky, E., Holland, E., Isaksen, I., Katima, J., Kirchhoff, V., Matson, P., Midgley, P. and Wang, M. 2001. Atmospheric chemistry and greenhouse gases. In: *Climate Change 2001: The scientific basis,* (eds. J. T. Houghton, et al.), Cambridge University Press, Cambridge, UK.

Flessa, H., Dörsch, P. and Beese, F. 1995. Seasonal variation of N_2O and CH_4 fluxes in differently managed arable soils in southern Germany. *J. Geophys. Res.* **100**, 23115–23124.

Geller, L. S., Elkins, J. W., Lobert, J. M., Clarke, A. D., Hurst, D. F., Butler, J. H. and Myers, R. C. 1997. Tropospheric SF6: Observed latitudinal distribution and trends, derived emissions and interhemispheric exchange time. *Geophys. Res. Lett.* **24**, 675–678.

Harnisch, J., Bischof, W., Borchers, R., Fabian, P., and Maiss, M. 1998. A stratospheric excess of CO_2 – due to tropical deep convection? *Geophys. Res. Lett.* **25**, 63–66.

Keeling, C. D., Piper, S. C. and Heimann, M. 1989. A three-dimensional model of atmospheric CO_2 transport based on obsrved winds: 4. Mean annual gradients and interannual variations. *Geophys. Monogr.* **55**, 305–363.

Kogubov, G. M. and Toskaev, A. I. 1999. *Forest of Komi respublik*. Dik Publishing House, Moscow, 460 pp.

Levin, I., Glatzel-Mattheier, H., Marik, T., Cuntz, M., Schmidt, M. and Worthy, D. E. 1999. Verification of German methane emission inventories and their recent changes based on atmospheric observations. *J. Geophys. Res.* **104**, 3447–3456.

Levin, I., Ciais, P., Langenfelds, R., Schmidt, M., Ramonet, M., Sidorov, K., Tchebakova, N., Gloor, M., N., Heimann, M., Schulze, E. D., Vygodskaya, N. N., Shibistova, O. and Lloyd, J. 2002. Three years of trace gas observations over the EuroSiberian domain derived from aircraft sampling – a concerted action. *Tellus* **54B**, this issue.

Lloyd, J., Langenfelds, R., Francey, R. J., Gloor, M., Tchebakova, N. M., Zolotukine, D., Brand, W. A., Werner, R., Jordan, A., Allison, C. A., Zrazhewske, V., Shibistova, O. and Schulze, E.-D. 2002. A trace gas climatology above Zotino, central Siberia. *Tellus* **54B**, this issue.

Matveev, L.T. 1984. *Rate of general meteorology and physics of the atmosphere*. Moscow State University Publishing House, Moscow, 518 pp.

Maiss, M. and Brenninkmeijer, C. A. M. 1998. Atmospheric SF_6: Trends, sources and prospects. *Environ. Sci. Technol.* **32**, 3077–3086.

Maiss, M., Ilmberger, J., Zenger, A. and Münnich, K. O. 1994. A SF_6 tracer study of horizontal mixing in Lake Constance. *Aquatic Sci.* **56**, 307–328.

Maiss, M., Steele, L. P., Francey, R. J., Fraser, P. J., Langenfelds, R. L., Trivett, N. B. A. and Levin, I. 1996. Sulfur hexafluoride - a powerful new atmospheric tracer. *Atmos. Environ.* **30**, 1621–1629.

Michkova, N. A. 1983. *Climate of the USSR*. Moscow State University Publishing House, Moscow, 365 pp.

Nakazawa, T., Sugawara, S., Inoue, G., Machida, T., Makshyutov, S. and Mukai, H. 1997a. Aircraft measurements of the concentration of CO_2, CH_4, N_2O, and CO and the carbon and oxygen isotopic ratios of CO_2 in the troposphere over Russia. *J. Geophys. Res.* **102**, 3843–3859.

Nakazawa, T., Ishizawa, M., Higuchi, K. and Trivett, N. B. A. 1997b. Two curve fitting methods applied to CO_2 flask data. *EnvironMetrics* **8**, 197–218.

Panikov, N. S. and Dedysh, S. N. 2000. Cold season CH_4 and CO_2 emissions from boreal peat bogs (West Siberia): Winter fluxes and thaw activation dynamics. *Global Biogeochem. Cycles* **14**, 1071–1080.

Prinn, R. and 16 others. 2000. A history of chemically and radiatively important gases in air deduced from ALE/GAGE/AGAGE. *J. Geophys. Res.* **105**, 17751–17792.

Ramonet, M., Ciais, P., Nepomnjashiy, I. L., Sidorov, K., Neubert, R., Picard, D., Kazan, V., Birand, S., Gusti, M., Kolle, O., Schulze, E. D. and Lloyd, J. 2002. Three years of aircraft based trace gas measurements over Fyodorovskoye southern taiga forest, 300 km north-west of Moscow. *Tellus* **54B**, this issue.

Schmidt, M., Graul, R., Sartorius, H. and Levin, I. 1996. Carbon dioxide and methane in continental Europe: a climatology, and ^{222}radon-based emission estimates. *Tellus* **48B**, 457–473.

Schmidt, M., Glatzel-Mattheier, H., Sartorius, H., Worthy, D. E. and Levin, I. 2001. Western European N_2O emissions – a top down approach based on atmospheric observations. *J. Geophys. Res.* **106**, 5507–5516.

Shibistova, O., Lloyd, J., Evgrafova, S., Savushkina, N., Zrazhewskaya, G., Arneth, A., Knohl, A., Kolle, O. and Schulze, E.-D. 2002. Seasonal and spatial variability in soil CO_2 efflux rates for a central Siberian *Pinus sylvestris* forest. *Tellus* **54B**, this issue.

Strunk, M., Engel, A., Schmidt, U., Volk, C. M., Wetter, T., Levin, I., and Glatzel-Mattheier, H. 2000. CO_2 and SF_6 as stratospheric age tracers: consistency and the effect of mesospheric SF_6-loss. *Geophys. Res. Lett.* **27**, 341–344.

Tans, P. P., Fung, I. Y. and Takahashi, T. 1990. Observational constraints on the global atmospheric CO_2 budget. *Science* **247**, 1431–1438.

Tans, P. P., Bakwin, P. S. and Guenther, D. W. 1996. A feasible Global Carbon Cycle Observing System: A plan to decipher today's carbon cycle based on observations. *Global Change Biol.* **2**, 309–318.

Weiss, R. F., Keeling, C. D. and Craig, H. 1981. The determination of tropospheric nitrous oxide, *J. Geophys. Res.* **86**, 7197–7202.

Worthy, D. E. J., Trivett, N. B. A., Hopper, J. F., Bottenheim, J. W. and Levin, I. 1994. Analysis of long range transport events at Alert, N.W.T., during the Polar Sunrise Experiment. *J. Geophys. Res.* **99**, 25329–25344.

Zimov, S. A., Semiletov, I. P., Davidov, S. P., Voropaev, Y. V., Prosyannikov, C. F., Wong, S. C. and Chan, Y. H. 1993. Wintertime CO_2 emission from soil of northeastern Siberia. *Arctic* **46**, 197–204.